

A New Method for PET Image Reconstruction Using Fourier-Wavelet Moment

Y. Hu¹, J. Zhou^{1,3}, H. Shu^{1,3}, L. Luo^{1,3} and J. L. Coatrieux^{2,3}

1. Laboratory of Image Science and Technology Southeast University, Nanjing 210096, China

2. Laboratoire Traitement du Signal et de l'Image-INSERM, Université de Rennes 1, Rennes, 35042, France

3. Centre de Recherche en Information Biomédicale Sino-français

Abstract—In this paper, a new non-regularization method for positron emission tomography (PET) reconstruction is proposed. The proposed method is a feature-based method using Fourier-Wavelet basis. In order to obtain the reconstructions, we have to calculate the Fourier-Wavelet moment (FWM) from the measurements. To achieve this, iterative method is employed. The rotation invariance property of the proposed basis permits us to reduce computational cost. A row-action (RA) like fast convergent algorithm is used to further accelerate the convergence rate. In experiment, we compare the proposed method with some existing algorithms. The results show that our method offers good reconstruction quality compared to conventional MAP method.

Key words: PET, reconstruction, moment, Fourier-Wavelet

I. INTRODUCTION

In positron emission tomography (PET) image reconstruction, statistical methods are widely used since Shepp and Vardi introduced MLEM method [9]. Because the problem of PET reconstruction is ill-posed, regularization methods are often used to improve reconstruction quality. To obtain good results, regularization term and parameters should be carefully chosen according to different situation. Such selection often involves interaction. Adaptation technique [4] can be applied to determine the regularization parameters whereas it increases the computational cost. Considering this, some literatures suggest using feature-based methods, which reconstruct image without using regularization terms.

Milanfar [5] applied Legendre moments to tomography reconstruction. He described a framework for the reconstruction of an image from the maximum likelihood (ML) estimates of its Legendre moments. However, Legendre polynomials are globally defined, as a result, it is not adequate for local feature extraction. Unlike Legendre polynomials, wavelet transform is capable of providing both time and frequency localization. The characteristic of wavelet transform is particularly suited to extract local features. Raheja [10] introduced the multigrid and multiresolution concept for PET image reconstruction using EM algorithm, and furthermore transforms his algorithm to a wavelet based multiresolution EM algorithm by extending the concept of switching resolutions in both image and data spaces. Lee [6] applied wavelet Shrinkage into EM algorithm, in his work, ordered subset (OS) method was employed to accelerate the convergence speed.

In this paper Fourier-Wavelet moments (FWM) are used for reconstruction. The FWM was introduced by Shen [8] with application to pattern recognition, it was shown that FWM has good performance in image characterization and is insensitive to noise. We establish the relationship between the measurements and the moments. Since FWM is rotation invariant, it can be used to reduce the computational cost. A row-action (RA) like block iterative algorithm is proposed to accelerate the convergence rate. In addition, inter-iteration filtering scheme is adopted to improve the reconstruction quality.

II. FWM AND RECONSTRUCTION MODEL

In the problem of positron emission tomography reconstruction, the ideal measurements are given by Radon transform:

$$y_{\theta}(s) = \int_0^1 \int_0^{2\pi} f(r, \phi) \delta(s - r \cos(\theta - \phi)) r dr d\phi \quad (1)$$

where $f(r, \phi)$ stands for isotopic distribution function, δ is the Dirac function. θ is the projection angle and s is the radial offset. In practice, θ and s take discrete values. We denote $\theta = \{\theta_i\}, i = 1, \dots, I; s = \{s_l\}, l = 1, \dots, L$, where I, L are number of projection angles and number of sampling per angle. The aim of reconstruction is to restore the distribution function (image) using the measurements $\{y_{\theta_i}(s_l) | i = 1, \dots, I; l = 1, \dots, L\}$.

The Fourier-Wavelet moment of an image, $f(r, \theta)$ is defined as [8] :

$$c_{m,n} = \int_0^1 \int_0^{2\pi} f(r, \phi) \psi_m(r) e^{-jn\phi} r dr d\phi \quad (2)$$

where $\psi_m(r)$ is wavelet basis function, m, n are integer numbers. Consider the family

$$\psi_{p,q}(t) = 2^{\frac{p}{2}} \psi(2^p t - q) \quad (3)$$

where p is a dilation parameter and q is a shifting parameter. In practice, we have the following mapping relation:

$$m = p(Q + 1) + q + 1 \quad (p = 0, \dots, P; q = 0, \dots, Q) \quad (4)$$

where P, Q are upper bound of p and q . Thus $\psi_m(r)$ can be replaced by wavelet basis functions $\psi_{p,q}(t)$. We consider

using the Mexican hat wavelets. In this case, the mother wavelet $\psi(r)$ is:

$$\psi(t) = \left(\frac{2}{\sqrt{3}} \pi^{-\frac{1}{4}} \right) (1-t^2) e^{-t^2/2} \quad (5)$$

Let:

$$\Psi_{m,n}(r, \phi) = \psi_m(r) e^{-jn\phi} \quad (6)$$

the distribution function can be approximated as follows:

$$f(r, \phi) \approx \sum_{m=1}^M \sum_{n=-N}^N c_{m,n} \Psi_{m,n}(r, \phi) \quad (7)$$

where $M = (P+1)(Q+1)$.

To reconstruct the distribution function, we need to establish the relationship between the measurements and the moments. Substituting (7) into (1), we have:

$$y_\theta(s) = \sum_{m=1}^M \sum_{n=-N}^N c_{m,n} \left\{ \int_0^1 \int_0^{2\pi} \Psi_{m,n}(r, \phi) \delta(s - r \cos(\theta - \phi)) r dr d\phi \right\} \quad (8)$$

Let:

$$A_{m,n}(s, \theta) = \int_0^1 \int_0^{2\pi} \Psi_{m,n}(r, \phi) \delta(s - r \cos(\theta - \phi)) r dr d\phi \quad (9)$$

equation(8) can be rewritten as:

$$y_\theta(s) = \sum_{m=1}^M \sum_{n=-N}^N c_{m,n} A_{m,n}(s, \theta), \quad (10)$$

It is easy to prove that $A_{m,n}(s, \theta)$ have the following properties:

Proposition 1: $\forall \theta \in [0, \pi)$, there are following relations:

$$\begin{aligned} A_{m,n}(s, \theta) &= e^{-jn\theta} A_{m,n}(s, 0) \\ A_{m,n}(s, \theta) &= \overline{A_{m,-n}(s, \theta)} \end{aligned} \quad (11)$$

where $\overline{A_{m,-n}(s, \theta)}$ is the complex conjugate of $A_{m,n}(s, \theta)$.

Define:

$$\mathbf{y}_\theta = [y_\theta(s_1), y_\theta(s_2), \dots, y_\theta(s_L)]^T \quad (12)$$

and $L \times M(2N+1)$ transform matrix:

$$\mathbf{A}(\theta) = \begin{bmatrix} A_{1,-N}(s_1, \theta) & \cdots & A_{M,N}(s_1, \theta) \\ A_{1,-N}(s_2, \theta) & \cdots & A_{M,N}(s_2, \theta) \\ \vdots & \ddots & \vdots \\ A_{1,-N}(s_L, \theta) & \cdots & A_{M,N}(s_L, \theta) \end{bmatrix}, \quad (13)$$

$$\mathbf{c} = [c_{1,-N}, c_{1,-N+1}, \dots, c_{1,N}, c_{2,-N}, \dots, c_{M,N}]^T \quad (14)$$

Equation (10) can be written in matrix form as:

$$\mathbf{y}_\theta = \mathbf{A}(\theta) \mathbf{c} \quad (15)$$

From Proposition 1, we may have Proposition 2:

Proposition 2: Let $\mathbf{E}(\theta)$ be $M(2N+1) \times M(2N+1)$ diagonal Matrix

$$\mathbf{E}(\theta) = \text{diag}\{e^{jN\theta}, \dots, e^{-jN\theta}, \dots, e^{jN\theta}, \dots, e^{-jN\theta}\} \quad (16)$$

then:

$$\mathbf{A}(\theta) = \mathbf{A}(0) \mathbf{E}(\theta). \quad (17)$$

(17) shows that $\mathbf{A}(\theta)$ is rotation invariant, which can be used to reduce the computational cost.

III. MODEL OPTIMIZATION

Equation (15) is the ideal model for the reconstruction problem, whereas in practice, the hard equality of (15) is no long true since the measurements are unavoidably noise contaminated. Usually, the measurements are assumed to be with Poisson statistics, however in modern PET scanning with random pre-correction, the measurements are no longer Poisson [7]. Fessler [3] suggested using Gaussian model for reconstruction, which has the following expression:

$$\mathbf{y}_{\theta_i} = \mathbf{A}(\theta_i) \mathbf{c} + \boldsymbol{\varepsilon} \quad (18)$$

where $\boldsymbol{\varepsilon}$ is a zero-means Gaussian vector, $\boldsymbol{\varepsilon} \sim N(0, \boldsymbol{\Sigma}_{\mathbf{y}_{\theta_i}})$, $\boldsymbol{\Sigma}_{\mathbf{y}_{\theta_i}}$ is covariance matrix with diagonal elements. To solve such model, we use weighted least square (WLS) method, the objective function is:

$$J(\mathbf{c}) = \arg \min_{\mathbf{c}} \sum_{i=1}^I \{ (\mathbf{y}_{\theta_i} - \mathbf{A}(\theta_i) \mathbf{c})^H \boldsymbol{\Sigma}_{\mathbf{y}_{\theta_i}}^{-1} (\mathbf{y}_{\theta_i} - \mathbf{A}(\theta_i) \mathbf{c}) \} \quad (19)$$

where the subscript H denotes the conjugate transpose. The weighting matrix $\boldsymbol{\Sigma}_{\mathbf{y}_{\theta_i}}$ plays a critical role, whose computation should be carefully performed to reflect real statistics feature of the measurements. Fessler [2] suggested performing $\boldsymbol{\Sigma}_{\mathbf{y}_{\theta_i}}$ as follows:

$$\boldsymbol{\Sigma}_{\mathbf{y}_{\theta_i}} = \text{diag}\{\max(\widetilde{\mathbf{y}}_{\theta_i}, \epsilon)\} \quad (20)$$

where $\widetilde{\mathbf{y}}_{\theta_i}$ is the unbiased estimator of the measurements, which we use a smooth version of measurements in our experiment, ϵ is a small threshold, which is set to be 5.0 in our paper.

Lots of methods can be used to solve the minimum of (19), among which we choose to use the successive approximation iteration method since the size of the involved matrix could be large. In order to accelerate the convergence speed, we decompose a full iteration into several sub-iterations each of which is carried out over one projection at a specific angular view. Such method is similar to the row-action technique [1]. With the help of proposition 2, we have the following iterative formula:

$$\begin{aligned} \mathbf{c}^{k,i+1} &= \mathbf{c}^{k,i} + \mathbf{E}(\theta_i) (\mathbf{A}(0)^H \boldsymbol{\Sigma}_{\mathbf{y}_{\theta_i}}^{-1} \mathbf{y}_{\theta_i} - \\ &\quad \mathbf{A}(0)^H \boldsymbol{\Sigma}_{\mathbf{y}_{\theta_i}}^{-1} \mathbf{A}(0) \mathbf{E}(\theta_i) \mathbf{c}^{k,i}) \end{aligned}$$

According to the definition of FWM, among the moments $\{c_{m,n} | m = 1, \dots, M, n = 1, \dots, N\}$, we get a group of wavelet coefficients from order 1 to M for a fixed value of n . Based on wavelet theory, finite order wavelet fitting can be used to suppress the noise effect. Similarly, we get a group



Fig. 1. Shepp-Logan phantom

of frequency component for a fixed value of m . Since high frequency signal are usually more sensitive to the noise, we can simply design a filter for the frequency component.

We propose the inter-iteration moment-filtering scheme: For each group of frequency component, define discrete Gaussian window $w_m(m = 1, \dots, M)$ with length of $2N + 1$ as follows:

$$w_m[d] = e^{-\frac{1}{2\sigma}(\frac{d-1-N}{N})^2}, d = 1, \dots, 2N + 1 \quad (21)$$

in which σ is the standard deviation that is proportional to the window width. A smaller value of σ produces a more narrow window that produces large suppress for those moments with higher harmonic order number. We choose Gaussian window just for its simplicity, other filters such as Hanning window and Blackman window can also be used.

The proposed filtering scheme can be performed by multiplying a weighting matrix \mathbf{W} .

$$\mathbf{W} = \text{diag}\{\mathbf{w}_1, \mathbf{w}_2, \dots, \mathbf{w}_M\} \quad (22)$$

Applying the filtering scheme into iteration, the complete algorithm is illustrated below:

- setup the initialization moments $\mathbf{c}^{0,1}$
- for each direction $i = 1, \dots, I$, repeat the following step

$$\begin{aligned} \mathbf{c}^{k,i+1} &= \mathbf{c}^{k,i} + \mathbf{E}(\theta_i)^H (\mathbf{A}(0)^H \Sigma_{\mathbf{y}_{\theta_i}}^{-1} \mathbf{y}(\theta_i) \\ &\quad - \mathbf{A}(0)^H \Sigma_{\mathbf{y}_{\theta_i}}^{-1} \mathbf{A}(0) \mathbf{E}(\theta_i) \mathbf{W} \mathbf{c}^{k,i}) \end{aligned} \quad (23)$$

- $\mathbf{c}^{k+1,1} = \mathbf{c}^{k,I+1}$
- stop if k reaches a prefixed value

In our experiment, the maximal number of iterations is set to 50.

IV. EXPERIMENTAL RESULTS AND ANALYSIS

A. Data Description

In our experiments, we used the Shepp-Logan phantom shown in Fig.1 to test the efficiency of different algorithms. The projection space was assumed to be 192 radial bins and 128 angles evenly spaced over 180° . The sinogram were globally scaled to a mean sum of 1,000,000 true events. The final reconstructed images were set to a size of 128×128 pixel matrices.

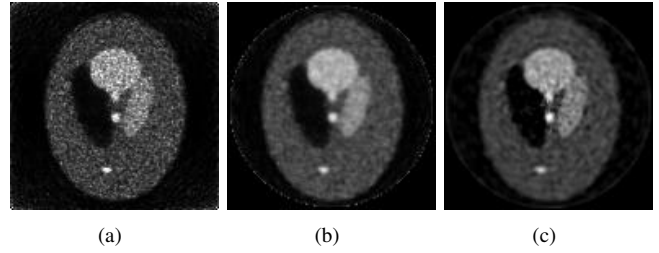


Fig. 2. reconstruction results using different methods: (a):MLEM ; (b):MAP ; (c):FWM ($\sigma=0.8$).

B. Results And Discussion

To evaluate the proposed method, the mean square error(MSE) is computed using the following definition:

$$MSE = \frac{\|f - f^*\|_2}{\|f^*\|_2} \times 100\% \quad (24)$$

in which f^* and f are isotopic distribution function and reconstruction result, $\|\cdot\|_2$ is the Euclidean norm of a vector.

We simulated the emission coincidence events during prompt windows and delayed windows respectively. The prompt data has to be modified to subtract the effects of the AC events. Taking these effects into account, the measured sinogram is generated based on the following recipes:

$$y_{s_l}(\theta_i) = Poisson(y_{s_l}^*(\theta_i) + a_{s_l}(\theta_i) + \zeta) - Poisson(a_{s_l}(\theta_i)) \quad (25)$$

where $y_{s_l}^*(\theta_i)$ is the ideal measurements value; $\zeta = 20\% \times \sum_{i=1}^I \sum_{l=1}^L y_{s_l}^*(\theta_i) / (IL)$ is the mean value of background noise; $a_{s_l}(\theta_i)$ is the number of coincident photon pairs collected in the delay windows, which we use $a_{s_l}(\theta_i) = 0.6 \times y_{s_l}^*(\theta_i)$ in our experiment; $y_{s_l}(\theta_i)$ is the final simulated measurements.

For comparison, MLEM, MAP and FWM methods are applied to reconstruct the distribution function (the MAP method used here is different from those under Poisson model, the details of the methods can be found in [3]). The MAP method is with Green's priori and the FWM method use 7 order discrete wavelets. The iteration number is 50 for each method. The reconstruction results are shown in Fig.2, and Fig.3 is the MSE curve of the different methods.

From Fig.2, we can see MAP method is superior to MLEM method in terms of noise suppression and can offer smoother image. The reconstruction quality of FWM method is close to MAP method. Furthermore, the convergence speed of FWM method is faster than MAP method as RA technique was applied. This can be seen from the descend speed of MSE curves.

Modifying parameter σ in (21), we can obtain different reconstruction results. Fig.4 shows results that different σ

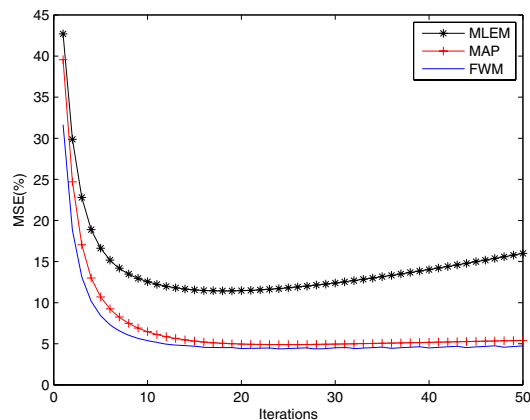


Fig. 3. MSE curves of different methods

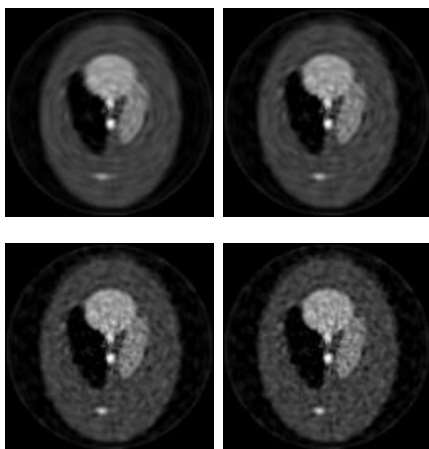


Fig. 4. FWM results with different parameters, $\sigma=0.2, 0.4, 0.8, 1.0$ from left to right, the corresponding MSE values are 5.15%, 5.01%, 4.88% and 5.04%.

were used for reconstruction. As we can see, the window width becomes larger as σ increases, thus the angular filtering effect is suppressed. In our experiments, we found the value between 0.8 and 1.0 is suitable because the details of the image are better reconstructed.

V. CONCLUSIONS AND FUTURE WORKS

In this paper, we proposed a new feature-based method for PET image reconstruction based on Fourier-Wavelet moments. Unlike the conventional MAP method, wavelet fitting coupled with filtering scheme are applied to suppress noise instead of employing regularization terms such as image priors. Thus neither interaction nor adaptation technique needs to be involved in the method. Meanwhile, the memory

cost of the proposed method is less than MAP method. Its reconstruction quality is close to MAP method. In further studies, we will apply our method to 3D PET reconstruction.

VI. ACKNOWLEDGMENTS

This research was supported by National Basic Research Program of China under grant, No. 2003CB716102, and Program for New Century Excellent Talents in University under grant No. NCET-04-0477.

REFERENCES

- [1] J. Browne and R. D. Pierro, "A row-action alternative to the EM algorithm for maximizing likelihoods in emission tomography", *IEEE Trans Medical Imaging*, vol. 15, no. 5, pp. 687-699, 1996.
- [2] J. A. Fessler, "Penalized weighted least-squares image reconstruction for positron emission tomography", *IEEE Trans. Medical Imaging*, vol.13, no. 2, pp. 290-300, 1994.
- [3] J. A. Fessler, H. Erdögan and W. B. Wu "Exact distribution of edge-preserving MAP estimators for linear signal models with Gaussian measurement noise", *IEEE Trans. Image Processing*, vol. 9, no. 6, pp.1049-1055, 2000.
- [4] N. P. Galatsanos and A. K. Katsaggelos "Methods for choosing the regularization parameter and estimating the noise variance in image restoration and their relation" *IEEE Trans. Image Processing*, vol 1, no. 3, pp. 322-336, 1992.
- [5] P. Milanfar, C. Karl and A. S. Willsky, "A moment-based variational approach to tomographic reconstruction", *IEEE Trans Image Processing*, vol. 5, no. 3, pp. 459-470, 1996.
- [6] N. Lee and Y. Choi, "A modified OSEM algorithm for PET reconstruction using wavelet processing", *Computerized Medical Imaging and Graphics*, vol 80, pp. 236-245, 2005.
- [7] V. Selivanov, Y. Picard and J. Cadorette, "Detector response models for statistical iterative image reconstruction in high resolution PET," *IEEE Trans. Nuclear Science*, vol. 47, no. 3, pp. 1168-1175, 2000.
- [8] D. Shen and H. Horace, "Discriminative wavelet shape descriptors for recognition of 2D patterns", *Pattern Recognition*, vol. 32, no. 2, pp. 151-165, 1999.
- [9] L. Shepp and Y. Vardi, "Maximization likelihood reconstruction for emission tomography", *IEEE Trans. Medical Imaging*, vol. MI-1, pp. 113-122, Oct. 1982.
- [10] A. Raheja and A. P. Dhawanb, "Wavelet based multiresolution expectation maximization image reconstruction algorithm for positron emission tomography", *Computerized Medical Imaging and Graphics*, vol 24, pp. 359-376, 2000.